Variability of the Compressive Strength of Parallel Strand Lumber

Sanjay R. Arwade[1]; Russell Winans[2]; and Peggi L. Clouston[3]

Abstract: Measurement of the compressive strength of parallel strand lumber (PSL) is conducted on specimens of varying size with nominally identical mesostructure. The mean of the compressive strength is found to vary inversely with the specimen size, and the coefficient of variation of the strength is found to decrease with increasing specimen size, and to be smaller than the coefficient of variation of strength for solid lumber. The correlation length of the compressive strength is approximately 0.5 m, and this correlation length leads to significant specimen-to-specimen variation in mean strength. A computational model is developed that includes the following properties of the PSL mesostructure: the strand length, the grain angle, the elastic constants, and the parameters of the Tsai-Hill failure surface. The computational model predicts the mean strength and coefficient of variation reasonably well, and predicts the correct form of correlation decay, but overpredicts the correlation length for compressive strength, likely because of sensitivity to the distribution of strand length used in the model. The estimates of the statistics of the PSL compressive strength are useful for reliability analysis of PSL structures, and the computational model, although still in need of further development, can be used in evaluating the effect of mesostructural parameters on PSL compressive strength.

DOI: 10.1061/(ASCE)EM.1943-7889.0000079

CE Database subject headings: Mechanics; Wood; Probability; Random processes; Simulation; Measurement; Compressive strength.

Author keywords: Mechanics; Wood; Strength; Probability; Random processes; Simulation; Composite lumber; Measurement.

Introduction

Structural composite lumber (SCL) is becoming an increasingly important building material as builders strive for sustainability, and as wood structures must provide adequate performance at larger scales in more challenging structural environments. The challenging design problems currently being addressed by timber design engineers were recently described in a series of articles and reports in *Structural Engineering International* (International Association of Bridge and Structural Engineers 2008), and the design of such high performance wood structures demands a more detailed examination of the mechanics of SCL. This paper describes tests conducted at the Univ. of Massachusetts, Amherst that characterize the compressive strength of parallel strand lumber (PSL), a type of SCL, and its variability. Attention is also given to determine whether the strength of PSL depends on the size of the member, and how the compressive strength varies spatially in a PSL member. A stochastic computational model based on a parallel system treatment and using the Tsai-Hill failure surface is also developed to predict the compressive strength of PSL.

PSL is a type of SCL that is composed of long narrow strands of wood that are often a by-product of the process of manufacturing plywood. The strands are adhesively bonded under high pressure, and the resulting material has a highly distinctive mesostructure (see Fig. 6 which is referenced again during description of the computational model), and very favorable mechanical properties, particularly a lower variability of both elastic modulus and strength. Although properties vary substantially between strands, the composite nature of the PSL mesostructure works to reduce levels of variability of the strength and elastic modulus to levels much lower than typically observed in solid wood.

One of the features of structural wood members is that they exhibit significant, correlated, variation of mechanical properties within members, in addition to between nominally identical members. Many standard reliability-based methods for assessing the safety of steel and concrete structural members do not account for this within-member variation, which strongly affects the reliability of wood structural members. Much of the previous research into variability of wood mechanical properties has focused on solid lumber, and is summarized in a very useful form in the *Wood Handbook* (Forest Products Laboratory 1999), which gives coefficients of variation for strength and modulus of about 20%. Spatial variation of both stiffness and strength of solid lumber has been observed experimentally, and stochastic models for this spatially correlated variation have been proposed. (Lam and Varoglu 1991a,b; Lam et al. 1994). Correlation lengths on the order of 10–100 cm were found in these studies. These studies provide an extremely useful framework for understanding the variability of PSL strength.

The computational model builds upon previous efforts by one

[1]Assistant Professor, Dept. of Civil and Environmental Engineering, Univ. of Massachusetts, 223 Marston Hall, Amherst, MA 01003 (corresponding author). E-mail: arwade@ecs.umass.edu

[2]Graduate Student, Dept. of Civil and Environmental Engineering, Cornell Univ., Ithaca, NY 14853. E-mail: rsw93@cornell.edu

[3]Associate Professor, Dept. of Natural Resources Conservation, Univ. of Massachusetts, Amherst, MA 01003. E-mail: clouston@nrc.umass.edu

Note. This manuscript was submitted on April 6, 2009; approved on August 13, 2009; published online on March 15, 2010. Discussion period open until September 1, 2010; separate discussions must be submitted for individual papers. This paper is part of the ***Journal of Engineering Mechanics***, Vol. 136, No. 4, April 1, 2010. ©ASCE, ISSN 0733-9399/2010/4-405–412/$25.00.

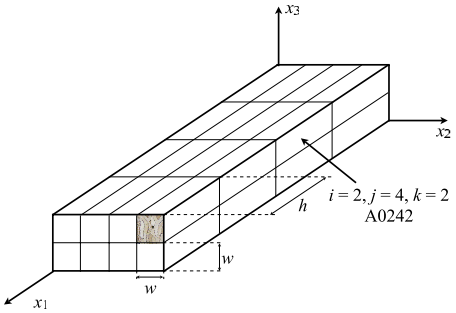

Fig. 1. Schematic illustration of compression specimen arrangement within larger PSL member. Arrangement shown is for A specimens, and the photograph of the PSL cross section is superimposed to indicate the orientation of the strands within the member.

of the writers (Clouston and Lam 2001, 2002; Clouston 2006) to develop finite-element models of SCL mesostructures that capture the variation in properties between strands and incorporate a reasonable model for the failure surface of the strands. Although stochastic models have been proposed for the mechanics of the PSL cross section (Bejo and Lang 2004), this is the first attempt to model the lengthwise features of the mesostructure. This paper also builds directly upon the writers' previous investigation of the variation of elastic modulus in PSL (Arwade et al. 2009).

Materials and Methods

The experiments consist of compression tests on stocky PSL specimens machined from larger PSL members. Two sets of specimens with different cross sectional area were tested to identify how cross section size affects strength variability. Fig. 1 shows schematically how the compression specimens were extracted from the larger PSL members.

Two groups of specimens, all with square cross sections with side length w, whose dimensions are shown in Table 1, were prepared and tested in this study. The symbol n_s denotes the approximate number of strands in each specimen. The A specimens are roughly one-half the cross-sectional area of the B specimens, and both sets of specimens have height h chosen in accordance with the compression testing requirements of ASTM standard D 143 (ASTM 2007). The constituent strands of the PSL are roughly aligned with the x_1 axis and have roughly 5 mm $\times$ 13 mm rectangular cross section. The specimens are identified as A_{ijk} and B_{ijk} where the indices denote the position of the specimen in the original PSL member. For example, B0921 was located at position $i=9$, $j=2$, and $k=1$ in the original member, and specimens B0921 and B1611 were separated by seven increments of 127 mm in the x_1 direction, by one increment of 39 mm in the x_2 direction and were located along the same x_3 specimen line. Note that the i index has two digits allocated to it. The A and B specimens were machined from members included in different shipments from the same manufacturer, Weyerhaeuser Company, Wash. All specimens were conditioned to the ambient room environment over several weeks in the Wood Mechanics Laboratory.

One issue that deserves discussion is the appropriate size for a representative volume element (RVE) for SCL. The A series specimens have a cross section that, although small, is slightly larger than that of secondary method specimens outlined in ASTM D 143 (25 mm $\times$ 25 mm). Based on this, the size was deemed adequate to fulfill the requirements of an RVE. Typical failure mechanisms for wood in compression were observed (i.e., crushing, wedge spilt, shearing, etc.) affirming the choice of A series specimen size.

Compression tests on all 64 A specimens and 162 B specimens were conducted in the Wood Mechanics Laboratory at the University of Massachusetts, Amherst using a universal material testing system operating in displacement control at a displacement rate of 0.25 mm/min to ensure test completion within 5–15 min. During testing the load was recorded digitally using a 147-kN load cell. Strains were measured using a digital extensometer with 25-mm gauge length. Each test was stopped when the postpeak load decreased to approximately 90% of the peak load.

These compression tests provide strength measurements dependent on specimen size. In the analysis of the experimental results it is assumed that the strength of each specimen represents the strength of the original member at the centroid of the compression specimen. For example, the measured strength of specimen A0732 provides a measurement of the strength of the original member at position $x_1=536$ mm, $x_2=70$ mm, and $x_3=42$ mm.

The original experimental design called for the measurement of both elastic modulus and strength of the PSL specimens. Testing revealed, however, that the inhomogeneity of PSL renders the measurement of elastic modulus through compression testing impractical; variation in properties led to localization of strain as measured by the extensometer. A reliable measurement of the average strain is required to estimate the elastic modulus of the specimen. If multiple extensometers were used in the experiment a better estimate of the average strain could be obtained, but this approach is cumbersome given the ease with which elastic modulus can be estimated using simple bending tests (Arwade et al. 2009).

Experimental Results

This section describes the results of the compression tests in the form of one and two point statistics of the specimen strength, and probability distributions for the specimen strengths. Fig. 2 shows typical stress-strain curves for the Group A and Group B tests. The curves for both groups illustrate strain variation due to the local nature of the strain measurement provided by the extensometer. This problem is also evident in the large scatter of slopes of the stress-strain curves in the elastic region and also the strain reversal that occurs near the end of the some of the traces. This strain reversal seemed to occur when a strand at the outer surface of the specimen began to split perpendicular to the grain, and then

Table 1. Specimen Parameters

Group	w (mm)	h (mm)	n_s	i range	j range	k range
A	28	82.5	12	1–8	1–4	1–2
B	39	127	24	1–18	1–3	1–3

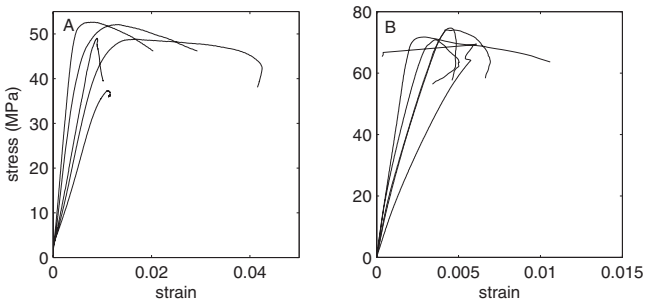

Fig. 2. Typical stress-strain curves for (a) Group A specimens; (B) Group B specimens

bow outward from the surface. This outward bowing led to local curvature of the surface and the observed strain reversal. Local damage near the surface occurred postpeak in many of the specimens, and tended to occur due to perpendicular-to-grain splitting rather than delamination at a strand interface. Many of these local failures were initiated near strand ends, at which point localized stress concentrations develop from the need to transfer load between strands. From here forward, only the peak stress, determined by dividing the peak load by the cross-sectional area of each specimen, is taken from the compression tests.

Fig. 3 shows histograms of the ultimate stress for the Groups A and B specimens, with the corresponding one-point statistics given in Table 2. The one-point statistics show that the strength of PSL has a lower coefficient of variation than does solid sawn lumber. The coefficients of variation are 15% for Group A and 12% for Group B, compared to 18% for solid sawn lumber (Forest Products Laboratory 1999). Furthermore, the standard deviation and coefficient of variation are both smaller for the Group B specimens than for the Group A specimens, although the 95% confidence intervals for the standard deviations (7.0, 9.3) and (6.7, 8.0) do overlap significantly.

The possible reduction in strength variance for the larger samples can be explained by the invocation of the central limit theorem since the constituent strands are ductile in compression so that the PSL strength is essentially the sum of the strand strengths. The difference in mean strength is 10 MPa with a 95% confidence interval of (7.75, 12.25) MPa, indicating that the mean strength of the A and B specimens are different with high likelihood. This difference has several possible explanations. The two specimen groups were extracted from members that were shipped several months apart, and would have been taken from different manufacturing runs. The results may also indicate a reverse size

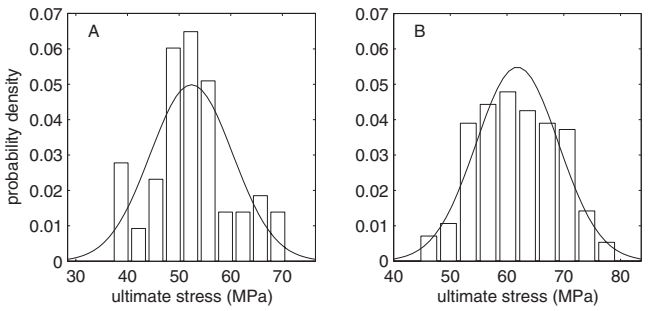

Fig. 3. Histograms with best fit Gaussian density for (a) Group A; (b) Group B specimens. Histograms based on 64 Group A specimens and 163 Group B specimens.

Table 2. One-Point Statistics of PSL Compressive Strength

Group	Mean (MPa)	Standard deviation (MPa)	Skewness	Kurtosis
A	52	8.0	0.34	2.9
B	62	7.3	0.045	2.3

effect in small samples of SCL loaded in compression. The idea of reverse size effect is at this stage purely conjectural since no physical mechanism is proposed. Although most pronounced in tensile failure modes for wood, modest size effects have been observed for wood in compression (Madsen 1990). The difference in the mean strengths between the specimen groups is likely due to their being extracted from different PSL structural members and is not inconsistent with normal variability of wood properties.

Finally, Kolmogorov-Smirnov tests cannot reject the hypotheses that the strengths are Gaussian, even at only 25% confidence levels. This result is in agreement with the skewness and kurtosis values being nearly 0 and 3. The best fit Gaussian densities are shown overlaid on the histograms in Fig. 3, and show general agreement with the data, although the number of specimens is too small to match very closely the exact density.

To investigate the spatial structure of PSL strength variability requires treating the compressive strength as a random field whose properties can then be estimated from the experiments. Let the compressive strength of the PSL member be denoted by $S(x,y,z)$. The compression tests cannot provide measurement of the strength at a point of infinitesimal dimension because the specimens must have a finite physical size to undergo mechanical testing. The measurement of strength by the testing of finite size specimens introduces spatial averaging of the properties so that the experiments provide measurements not of $S(x,y,z)$ but rather of $\bar{S}(x,y,z)$, which represents the strength field filtered through the averaging operation of the compression tests. Furthermore, experimental determination of strength also introduces noise, or experimental error, into the measurements. Therefore, what is actually obtained by the experiments is a set of observations $\hat{\bar{S}}_{ijk} = \hat{\bar{S}}(x_i, y_j, z_k)$, where the hat represents the presence of noise in the observations. Simulations not described in detail here indicate that the spatial averaging effect is small, and analysis of the experimental results indicates that the experimental noise is small relative to the actual fluctuations of the strength. Henceforth, therefore, we denote the measured strengths by S.

Each compression test is considered to provide an observation of $S(x,y,z)$ at the centroid of the specimen. Making reference to the coordinate system defined in Fig. 1 the compression test of specimen A_{ijk} gives a measurement of $S_{ijk}=S[(h/2)+(i-1)h,\ (w/2)+(j-1)w,\ (w/2)+(k-1)w]$. Fixing the j and k indices provides observations $s_{jk}(x)$ of the random process $S_{jk}(x)$. These observations are shown in Fig. 4. One observation that can be made, particularly with respect to Group A specimens, is that these specimens are not long enough to capture long period variations in the strength process. Another way of stating this observation is that the means of the individual specimens are not identical. If the specimens are long compared to the longest period component of the random process, and if the underlying process is ergodic, then the sample means should converge to the true mean of the process. Furthermore, and what is more important for strength analysis, the minimum strength in each specimen is dif-

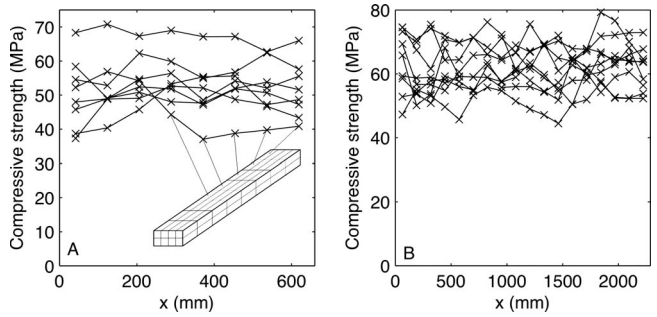

Fig. 4. Experimental observations of the strength random processes $S_{jk}(x)$ for (a) Group A specimens; (b) Group B specimens

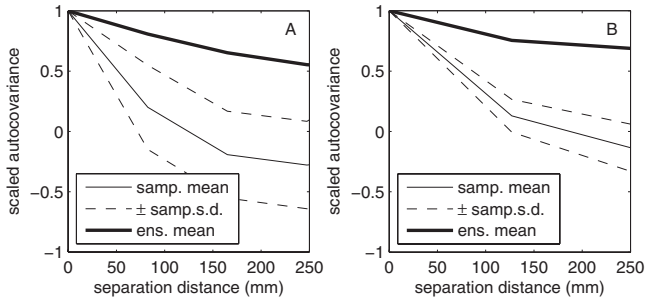

Fig. 5. Sample and ensemble estimates of the scaled autocovariance for (a) A specimens; (b) B specimens. The heavy solid line is the ensemble estimate, and the dashed lines indicate the mean sample estimate plus and minus one standard deviation.

ferent, again because of the relatively short length of the specimens.

Table 3 shows statistics for each of the experimentally obtained samples of $S(x)$. For both the A and B specimens the sample standard deviations are substantially lower than the ensemble standard deviation, indicating again that the specimens are of insufficient length to fully capture strength variation. Quantitatively, the sample standard deviations for the A specimens contribute only approximately 28% of the total ensemble variation, whereas for the B specimens the contribution is approximately 27%. The similarity of these percentages indicates that the correlation length for the two specimens, despite their different cross-sectional dimensions, is similar.

The final element of the second moment characterization of the strength process consists of the spatial correlation or covariance functions. Assuming that the strength process is at least weakly stationary, the scaled autocovariance is defined by

$$\rho(\Delta x) = \frac{(S(x) - E[S])(S(x+\Delta x) - E[S])}{\sigma_S^2} \tag{1}$$

where $E[\cdot]$=expectation operator; Δx=separation distance; and σ_S^2=variance of $S(x)$.

The scaled autocovariance takes values in the interval $[-1,1]$ and can be estimated from data by estimating the expectations either by ensemble averaging or spatial averaging. In the case where the process is ergodic, the sample and ensemble estimates converge to the exact autocovariance. Fig. 5 shows the sample and ensemble estimates of the scaled autocovariance of the A and B specimens, and illustrates the difference between the sample and ensemble estimates that is characteristic of estimates made from a suite of samples that is short relative to the correlation length of the stochastic process.

Assuming an exponential form $\rho(\Delta x)=\exp(-\lambda\Delta x)$ for the decay of covariance with Δx specified in millimeters, least-squares fitting gives the parameters shown in Table 4, namely the decay parameter λ and the correlation length L_c. The results show a somewhat longer correlation length for the larger B specimens, and correlation lengths between 0.4 and 0.6 m. These correlation lengths are shorter than those found for the elastic modulus, which were found in a previous study (Arwade et al. 2009) to be approximately 1 m. That the strength stochastic process should have shorter correlation length than the elastic modulus process is consistent with the increased sensitivity of strength to random defects in the PSL mesostructure.

The experimental results described earlier provide a full characterization of the compressive strength stochastic process $S(x)$, which is estimated to be Gaussian with mean, variance, and scaled autocovariance as described earlier. The characterization can be used to generate samples using any of the standard methods for simulation of Gaussian stochastic processes, and these samples can be used in Monte Carlo simulation of the response of PSL structures.

Table 3. Specimen-by-Specimen Statistics of PSL Strength Random Process

Specimen	Mean (MPa)	Standard deviation (MPa)	Specimen	Mean (MPa)	Standard deviation (MPa)
A1	48	4.8	B1	71	3.9
A2	46	7.8	B2	69	4.3
A3	52	3.4	B3	60	4.8
A4	50	2.5	B4	68	3.4
A5	58	3.6	B5	63	4.1
A6	67	2.4	B6	56	4.1
A7	51	3.5	B7	59	3.6
A8	47	6.6	B8	57	2.4
			B9	51	3.6
Means	—	7.7	Means	—	6.6
Standard deviations	4.3	—	Standard deviations	3.8	—

Table 4. Parameters of Exponential Autocovariance Functions for A and B Specimens

Specimen group	λ	L_c (mm)
A	0.0026	390
B	0.0017	600

Computational Model

Mesostructural Geometry

Fig. 6 shows a photograph of a short length of a typical Group A specimen and the idealized strand mesotructural geometry used in generating the computational model described here. A reference coordinate system is established relative to the specimen geometry. The key assumptions made in developing the idealized mesostructural geometry are that:

1. All strands are rectangular prisms with long edge aligned with the long edge of the test specimen;
2. Strand cross section dimensions are deterministic and constant giving a strand cross-sectional area A_s;
3. No voids exist in the PSL;
4. The interfaces between the strands are perfectly bonded, and have zero thickness; and
5. Grain orientation is defined by the single random angle Θ.

In this mesostructural model each strand has two geometric variables associated with it, its length and grain angle. These will both be treated as random variables according to models described in the next section.

Strand Mechanics

The strands are assumed to have an orthotropic elastic constitutive matrix with one of the principal material axes aligned with the reference x_3 coordinate, and the orientation of the other two, orthogonal principal material axes determined by the grain angle Θ. The assumptions made about the strand geometry and orientation of the strands relative to the reference coordinate system allow use of the 2D plane stress assumption for the response of each strand. Under plane stress assumptions the constitutive matrix C of each strand is defined by two elastic moduli $E_{1'}$ and $E_{2'}$, a Poisson's ratio $\nu_{1'2'}$, and a shear modulus $G_{1'2'}$. Here the x_1' axis is defined relative to the reference x_1 axis by the grain orientation angle Θ. The constants are modeled as independent Gaussian random variables truncated at zero to avoid negative values. The constitutive matrix C is assumed to be constant within a given strand.

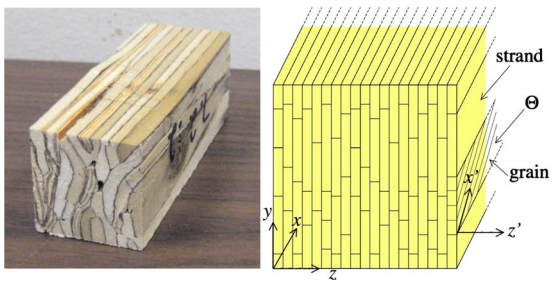

Fig. 6. Actual and idealized PSL mesostructure

The postelastic response of the strands is assumed to be perfectly plastic with no strain hardening. The Tsai-Hill failure surface is a commonly accepted model for wood and is used here. The failure surface is given in strand coordinates by

$$\left(\frac{\sigma_{11}'}{F_1'}\right)^2 + \left(\frac{\sigma_{22}'}{F_2'}\right)^2 - \left(\frac{\sigma_{11}'\sigma_{22}'}{F_1'^2}\right) + \left(\frac{\sigma_{12}'}{S_{12}'}\right)^2 = 1 \tag{2}$$

In the preceding expressions F_i is the uniaxial failure stress in the x_i direction and S_{ij} is the shear failure stress. Note that the primes on the quantities in the preceding expressions indicate that the quantities are expressed in the strand coordinate system. Therefore, checking whether a given strand has failed under a given compressive stress requires transformation of the stress tensor to the strand coordinate system.

The material model for each strand, assuming two dimensional behavior, contains four parameters for the elastic response, $E_{1'}$, $E_{2'}$, $\nu_{1'2'}$, and $G_{1'2'}$, and three parameters defining the yield surface $F_{1'}'$, $F_{2'}'$, and $S_{1'2'}'$. Each of these parameters, expressed in the strand coordinate system, is treated as a random variable according to models described in the following section.

Cross Section Mechanics

A simple method can be used to predict the compressive strength of a PSL cross section composed of strands with varying grain angles, deterministic cross sectional area, orthotropic elastic response, and perfectly plastic postelastic response with yielding determined using the Tsai-Hill criterion. The prediction method treats the strands as parallel elements in a system that fails only when all elements in the system have failed. The key assumptions in this predictive model are that:

1. The state of strain is uniaxial and identical in all strands; and
2. All strands are sufficiently ductile that cross section failure occurs only when all strands have reached their limiting load.

Given the PSL mesostructural model described earlier a cross section is defined by a number of constituent strands n_s, the deterministic strand cross sectional area A_s, the random grain angles Θ_i, the random elastic constitutive matrices C_i, and the random vectors $D_i=[F_{1'}', F_{2'}', S_{1'2'}']^T$ that contain the parameters of the 2D Tsai-Hill failure surface for each strand expressed in strand coordinates. The grain angle and orthotropic elastic constitutive matrix can be used to calculate the effective elastic modulus

$$\bar{E}_1 = f[C(\Theta)] \tag{3}$$

in the x_1 direction. Using the effective modulus shown earlier and the Tsai-Hill failure surface, the value of uniaxial strain at which a strand fails can be calculated. Denote this strain as ϵ_y. To simulate the compression tests performed in the experimental part of this project, a simulated loading $\epsilon_1=\epsilon_1(t)$ is applied. Here, t should not be interpreted as real time, but simply as an index for the incremental application of strain during the nonlinear analysis of the strand cross section.

The cross section analysis procedure is as follows:

1. For each strand, calculate the effective elastic modulus $\bar{E}_{1,i}$;
2. For each strand, calculate the applied uniaxial strain $\epsilon_{y,i}$ at which the strand reaches the Tsai-Hill failure surface;
3. Sort the yield strains so that $\epsilon_{y,i} < \epsilon_{y,i+1}$;
4. At each point $\epsilon_{y,i}$ in the applied strain history, calculate for each strand the x_1 directed normal stress $\sigma_{11,ij}, j=1,\ldots,n_s$ by

$$\sigma_{11,ij} = \min\{E_{1,j}\epsilon_{y,i}, E_{1,j}\epsilon_{y,j}\} \tag{4}$$

5. At each point $\epsilon_{y,i}$ in the applied strain history calculate the average cross section stress

$$\bar{\sigma}_{11,i} = \frac{1}{n_s}\sum_{j=1}^{n_s} \sigma_{11,ij} \tag{5}$$

6. Construct the cross section stress-strain curve by starting from the origin and linearly interpolating the points $(\epsilon_{y,i}, \bar{\sigma}_{11,i})$.

Note in the preceding procedure that the Tsai-Hill failure surface is expressed in strand coordinates so that the stresses resulting from the applied strain must be transformed into the strand coordinate system before checking for failure to determine $\epsilon_{y,i}$. The preceding procedure gives the nonlinear stress-strain curve for the cross section. If only the strength, or ultimate stress of the cross section is desired this can be calculated directly by

$$\bar{\sigma}_u = \sum_{j=1}^{n_s} \bar{E}_{1,j}\epsilon_{y,j} = \max_{i=1,\ldots,n_s} \{\bar{\sigma}_{11,i}\} \tag{6}$$

Model Validation

To validate the computational model described earlier a series of simulations were made that were designed to replicate as closely as possible the physical experiments. The simulations use geometric parameters chosen to match those used in the physical tests, and models for the random geometric, elastic, and strength parameters that are based on published quantification of parameter uncertainty in wood.

Specimen Geometry and Sample Sizes

The validation simulations are divided into two groups, labeled A′ and B′ to correspond to the A and B experimental specimen groups. The A′ specimens are square in cross section with side length of 28 mm and length of 660 mm, are composed of 12 strands of dimension 13 mm by 5 mm. The B′ specimens also have square cross section but are larger, with side length of 39 mm and length of 2.286 m, and are composed of 24 strands of dimension 13 mm by 5 mm. Ten independent realizations of A′ and B′ specimens are generated using the mesostructural model described earlier, and, using the proposed computational model, the strength of each cross section in each specimen is calculated. The ten realizations used in the simulation are similar to the number of specimens used in the experimental program. This procedure provides realizations of the strength random process $S(x)$. For validation purposes, these realizations are compared statistically to the experimentally obtained realizations of $S_{jk}(x)$. Here, it is assumed that the effect of spatial averaging of the strength, indicated by the overbar on S, is negligible.

Probabilistic Models for Random Parameters

The computational model for PSL strength contains nine random parameters for each strand, the grain angle and length, four elastic constants, and three strength constants. The grain angle is treated as a random variable drawn from the probability mass function (pmf) shown in Fig. 7. This experimentally determined pmf for the grain angle indicates that the grain of most strands is well aligned with the longitudinal axis of the PSL member.

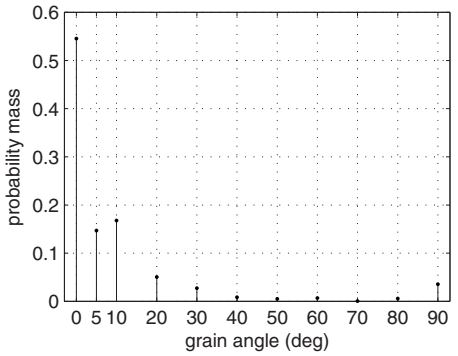

Fig. 7. Probability mass function for grain angle adopted from (Clouston 2006). Grain angle of 90° corresponds to a knot defect.

The strand length is a critical parameter in defining the PSL mesostructural model because the end of individual strands determines when the properties of the cross section change. This is because the current model neglects spatial variation of the elastic constants, grain angle, and yield surface constants within a strand. Here, the strand length is modeled as a random variable

$$L_s = 0.610 + 1.82Z \tag{7}$$

in which Z=β-distributed random variable with parameters β and α. The strands have length distributed in the interval (0.610 m, 2.43 m) in with an expected value in meters of $\langle L_s \rangle = 0.610 + 1.82[\alpha/(\alpha+\beta)]$. This is consistent with the manufacturing process of the strands in which the strands are generated during the processing of logs into 2.44-m-long sheets of plywood.

The elastic constants and parameters of the yield surface are modeled as Gaussian random variables with mean values and coefficients of variation based on published measurements of strength and elastic properties of solid dimensioned lumber. The parameters of these models are given in Table 5 and represent approximately 20% variation of most of the elastic and strength properties.

Table 5. Probability Model Parameters for Strand Elastic Properties and Strength

Property	Mean value	Coefficient of variation
$E_{1'}$	13 GPa	0.20
$E_{2'}$	0.82 GPa	0.20
$\nu_{1'2'}$	0.02	0
$G_{1'2'}$	0.88 GPa	0.20
$F'_{1'}$	57 MPa	0.20
$F'_{2'}$	10 MPa	0.20
$S'_{1'2'}$	12 MPa	0.20

Table 6. One-Point Statistics of PSL Compressive Strength for Validation Sets

Group	Mean (MPa)	Standard deviation (MPa)	Skewness	Kurtosis
A′	54	5.6	0.10	2.1
B′	55	3.7	−0.08	2.6

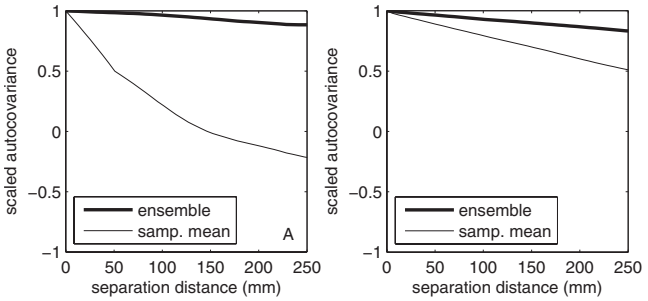

Fig. 8. Sample and ensemble estimates of the scaled autocovariance of PSL strength estimated from simulations generated from the proposed computational model: (a) A′ specimens; (b) B′ specimens

Validation Results

The validation sets A′ and B′ have point statistics (Table 6) that agree reasonably well with the experimental statistics (Table 2). Notable differences between the experimental and validation data are that in the experiments, the B set has a higher mean strength than the A set and that the standard deviations of strength are lower in the simulated A′ and B′ sets than in the experimental sets. The higher standard deviation observed in the experimental strengths is not unexpected since the computational model in its current state does not consider the effect of voids and knot defects in the specimen. Furthermore, the adhesive phase that bonds the strand interfaces is not modeled, and the interfaces are assumed to be perfectly bonded. If deformation occurs at the strand interfaces unequal strain distribution could arise in the composite, thereby increasing the variability of the cross section strength. Efforts to include these effects are ongoing by the writers. On the whole, the accuracy of the predictions of the mean value of the compressive strength is satisfactory given the large natural variation in wood mechanical properties. The predictions of standard deviation are lower than observed experimentally, and the standard deviation of strength is inversely related to the cross-sectional size. The difference between the standard deviations of the A′ and B′ samples is statistically significant using the 95% confidence intervals (4.9, 6.5) and (3.4, 4.1), respectively.

Although the predictions of the standard deviation of the compressive strength are lower than those found from the experiment, the computational model does predict to a reasonable degree of accuracy the reduction in standard deviation of strength induced by the increase in cross section size and number of constituent strands from the A to B and A′ to B′ specimens.

Fig. 8 shows the ensemble and mean sample scaled autocovariance functions for the simulated A′ and B′ specimens. A comparison with Fig. 5 shows that the computational model generates sample PSL mesostructures with substantially slower correlation decay. This finding points to the absence of some sources of spatial fluctuation of strength in the computational model. The most likely explanation of the more rapid decay of autocovariance in the experimental specimens is that the strands are shorter than what has been assumed in the validation specimens.

Specifically, the mean strand length in the A′ and B′ specimens is 2.3 m, quite near the upper limit of strand length, and giving a correlation length for the B′ specimens of 0.9 m. If the mean strand length is reduced to 1.15 m, the correlation length for specimens of the same cross-sectional size as the B′ specimens become 0.65 m. Although it would be possible to choose parameters of the strand length distribution so that the scaled autocovariance functions of the simulated specimens more closely match those found experimentally, a better approach is to determine the appropriate distribution of strand length by experimental characterization of the material. This work is currently being undertaken by the writers, but is considered beyond the scope of this paper, in which the primary aims are the experimental characterization of the spatial variation of strength and the demonstration that the proposed computational model captures the salient features of the mechanics of PSL.

The stochastic computational model introduced here is effective at predicting the mean value and standard deviation of compressive strength of PSL, although the standard deviation is somewhat underpredicted due to the absence of voids and defects from the model. Inclusion of these features is the subject of ongoing research. The stochastic computational model predicts scaled autocovariance functions of the compressive strength that exhibit substantially slower decay than observed experimentally. The most likely source of this discrepancy is the assumed distribution of strand lengths. In the absence of an experimental characterization of this distribution, the subject of ongoing research, the computational model should not be considered validated for prediction of longitudinal correlation of strength, although it may still be useful as a tool for studying the effect of parameter variation on the spatial variation of PSL strength.

Conclusions

Compression tests on PSL specimens machined from a larger PSL member are used to characterize the mean value, standard deviation, and spatial variability of the compressive strength of PSL. By tracking the original location of the test specimens within the original member the compression tests are used to construct observed samples of the stochastic process representing the compressive strength along the length of a PSL member.

Tests consisted of 64 specimens with 28 mm by 28 mm cross section and 162 specimens with 39 mm by 39 mm cross section. The larger specimens are found to have higher strength than the smaller specimens, and lower standard deviation. The finding of higher strength in the larger specimens is not easily explained by current understanding of PSL mechanics, but it must be noted that the specimens came from different shipments of material, and were conditioned only to ambient room conditions. Although the experimental results show a lower standard deviation of strength for the larger samples the 95% confidence intervals for the estimates of the standard deviations do overlap significantly. A reduction in strength variability with cross section size is, however, predicted by computational modeling of PSL mechanics. A Gaussian model is found to be suitable, according to a Kolmogorov-Smirnov test, to the strength data. Suitability of a Gaussian model is unusual for a material strength, but is reasonable for PSL in compression since material ductility ensure that the cross section strength is essentially a sum of the strength of the constituent strands.

There is persistent lengthwise correlation in the strength stochastic process with correlation lengths of roughly 0.5 m. These correlation lengths are long enough that significant variation would be expected in the mean strength of nominally identical PSL members of lengths used in common constructions.

A computational model for the compressive strength of PSL is introduced in which the strand length, grain angle, orthotropic elastic constants, and parameters of the Tsai-Hill failure surface are treated as independent random variables with parameters calibrated to known properties of solid wood. The computational

model treats PSL as a parallel system of strands, and assumes elastic-perfectly plastic behavior for each strand. The computational model provides valid predictions of the mean strength and slightly underpredicts the standard deviation of strength, although it does predict the reduction in strength variation with increasing cross section size. The computational model significantly overpredicts the correlation length of compressive strength, but the correlation length is found to be highly sensitive to the distribution of strand lengths. Nevertheless, the current computational model should be immediately useful in predicting the mean and standard deviation of PSL compressive strength for different size members and members with strands from a variety of species, and the form of the correlation decay matches that found in the experiments. The probabilistic characterizations of the PSL strength presented in this paper provide the necessary data to embark upon thorough studies of the structural reliability of PSL members and structures that incorporate spatial variation of the compressive strength of the material.

Acknowledgments

This work was partially supported by the National Science Foundation through Grant CMMI-0926265.

References

Arwade, S., Clouston, P., and Winans, R. (2009). "Measurement and stochastic computational modeling of the elastic properties of parallel strand lumber." *J. Eng. Mech.*, 135(9), 897–905.

ASTM. (2007). "Standard test methods for small clear specimens of timber." *ASTM D143-94*, West Conshohocken, Pa.

Bejo, L., and Lang, E. (2004). "Simulation based modeling of the elastic properties of structural composite lumber." *Wood Fiber Sci.*, 36, 395–410.

Clouston, P. (2006). "Characterization and strength modeling of parallel strand lumber." *Holzforschung*, 61, 392–399.

Clouston, P., and Lam, F. (2001). "Computational modeling of strand-based wood composites." *J. Eng. Mech.*, 127(8), 844–851.

Clouston, P., and Lam, F. (2002). "A stochastic plasticity approach to strength modeling of strand-based wood composites." *Compos. Sci. Technol.*, 62, 1381–1395.

Forest Products Laboratory. (1999). *Wood handbook: Wood as an engineering material*, USDA, Madison, Wis.

International Association of Bridge and Structural Engineers. (2008). "Special issue: Tall timber buildings." *Struct. Eng. Int. (IABSE, Zurich, Switzerland)*, 18(2), 133–136.

Lam, F., and Varoglu, E. (1991a). "Variation of tensile strength along the length of lumber part 1: Experimental." *Wood Sci. Technol.*, 25, 351–359.

Lam, F., and Varoglu, E. (1991b). "Variation of tensile strength along the length of lumber part 2: Model development and verification." *Wood Sci. Technol.*, 25, 449–458.

Lam, F., Wang, Y.-T., and Barrett, J. D. (1994). "Simulation of correlated non-stationary lumber properties." *J. Mater. Civ. Eng.*, 6(1), 34–53.

Madsen, B. (1990). "Length effects in 28mm spruce-pine-fir dimension lumber." *Can. J. Civ. Eng.*, 17(2), 226–237.